The influence of thermal contact resistance on the thermal history in laser-assisted fiber placement

Celik, O.; Amin Hosseini2, S.M.; Baran, İsmet; Grouve, Wouter J B; Akkerman, Remko; Peeters, D.M.J.; Teuwen, Julie J.E.; Dransfeld, C.A.

THE INFLUENCE OF THERMAL CONTACT RESISTANCE ON THE THERMAL HISTORY IN LASER-ASSISTED FIBER PLACEMENT

Ozan Çelik[1,*], S. M. Amin Hosseini[2], İsmet Baran[2], Wouter J. B. Grouve[2], Remko Akkerman[2], Daniël M. J. Peeters[1], Julie J. E. Teuwen[1], Clemens A. Dransfeld[1]

[1] Aerospace Structures and Materials, Faculty of Aerospace Engineering, Delft University of Technology, 2629 HS, Delft, The Netherlands
[2] Chair of Production Technology, Faculty of Engineering Technology, University of Twente, 7522 NB, Enschede, The Netherlands
[*]Corresponding author. E-mail: ozan.celik@tudelft.nl

ABSTRACT

The temperature history during the laser assisted fiber placement (LAFP) process is very important since it significantly influences the final quality of the structure. Air pockets between subsequent plies, caused by the lack of intimate contact, act as insulators and reduce the through-thickness heat transfer. This phenomenon is commonly referred to as the inter-ply thermal contact resistance (TCR). So far, the link between the degree of intimate contact, the corresponding TCR and its influence on the thermal history has not been clearly demonstrated specifically for LAFP. The results indicate that TCR influences the cooling period of the process.

1. INTRODUCTION

Laser-assisted fiber placement (LAFP) is a production method which is suitable for manufacturing typical aerospace components in an automated fashion. In-situ (without a post-consolidation step in an autoclave, oven or press) consolidation is achievable with LAFP using thermoplastic composite materials. This provides potential reduction in cycle time, energy consumption and cost. In addition, optimized structures can be manufactured by steering fibers and material waste can be reduced by producing near net shape components. In modern LAFP systems, a laminate is built by heating the surface of the tape and substrate with a laser heat source pointed towards the nip point and compacting with a flexible roller as shown in Figure 1.

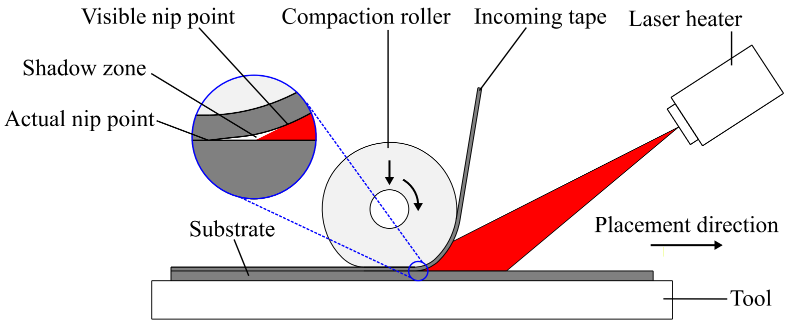

Figure 1. Schematic description of LAFP systems.

During LAFP, temperature history is one of the main drivers for a number of phenomena that determine the final part quality such as intimate contact, healing, void compaction/decompaction, crystallinity evolution, and residual stresses. It is affected by several process parameters such as the laser power, laser angle, spot size and placement speed.

Apart from these process parameters, lack of intimate contact at the interfaces of the laminate might have an influence on the temperature history. Air pockets between subsequent plies act as insulators and reduce the through-thickness heat transfer. This phenomenon is commonly referred to as the inter-ply thermal contact resistance (TCR).

Typically, the thermal models of the LAFP process are built on the assumption of perfect intimate contact between the compacted tape and the substrate [1–3]. This assumption was not supported with experimental data regarding the degree of intimate contact at the interfaces of the laminate. Only a few studies in the literature examined the effects of TCR during LAFP experimentally [4,5]. So far, thermocouples embedded in the substrate were used. Contact temperature measurement methods are questionable in this case, since they affect the intimate contact in their surroundings directly. Moreover, insulation material and voids around the thermocouple add more ambiguity to the obtained data. This is why this effect must be investigated with an alternative, and preferably non-contact, temperature measurement method.

The aim of this study is to investigate the effect of TCR (and the related degree of intimate contact) on the temperature history during LAFP with a non-contact method considering the actual microstructure of the laminate. Laminates with different degrees of intimate contact were manufactured by changing only the compaction force and keeping all other parameters, such as the laser power/angle and placement speed, constant. During placement, the temperature at the roller exit was measured with an infrared camera which was mounted to the rear side of the placement head. Following the production with different compaction forces, cross-sectional micrographs were taken from the samples and the degree of intimate contact was determined. The temperature at the roller exit and the cooling behavior after compaction were compared with the measured degree of intimate contact. These findings will lead to a more accurate thermal analysis of the LAFP process.

2. EXPERIMENTATION

2.1 Fiber Placement System and Specimen Manufacturing

The specimens were manufactured at Royal Netherlands Aerospace Center (NLR). A six-axis articulated robot on a linear axis provided by Coriolis was used. The machine was able to deliver eight 6.35 mm (1/4 in.)-wide tapes simultaneously up to 800 mm/s placement speed. The end effector was equipped with a 6 kW Laserline LDF series diode laser system and an optic lens which created a 56 mm× 28 mm rectangular illuminated area at the 250 mm focal distance. A conformable compaction roller with 60 shore hardness and a diameter of 70 mm was installed on the machine. For this study, a second thermal camera was mounted to the rear side of the machine in addition to the front thermal camera which is commonly used for process control as shown in Figure 2.

The material used in this study was Toray TC1200 AS4/PEEK tapes (fiber volume fraction 59 %, melting temperature 343 °C) in 6.35mm-wide slit form. The thickness of the prepreg was 0.15 mm. First, 1000 mm-long, $[0]_5$ substrates were placed for each specimen depositing only the odd tows instead of all eight tows. This was done to reduce the laminate width so that loss of contact with the table due to warpage can be limited. Additionally, the pressure over the width of the compaction roller was kept uniform by depositing four odd tows (Tow 1-3-5-7) simultaneously. The laser power was set to 1500 W for the first layer and 1750 W for the remaining four layers. The compaction force was set to 500 N. These parameters were determined based on earlier experience. Then, the sixth layer of each specimen was placed with a combination of each laser power and compaction force in Table 1.

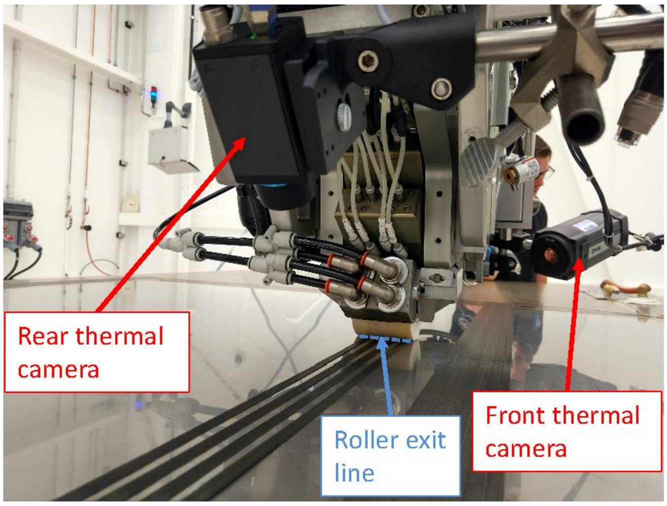

Figure 2. Front and rear thermal cameras on the fiber placement machine to measure the tape inlet and exit temperatures during the process.

Table 1. Process parameters used for manufacturing the samples.

Experiment No.	Laser Power (W)	Compaction Force (N)
1	1300	100
2	1300	500
3	1300	1000
4	1500	100
5	1500	500
6	1500	1000
7	1750	100
8	1750	500
9	1750	1000

2.2 Process Temperature Measurement

A FLIR SC325 (320×240 pixel-resolution, calibrated in the 200-1200 °C range to ± 2 °C or ± 2%) and a FLIR A35 (320×256 pixel-resolution, calibrated in the -40-550 °C range to ± 5 °C or ± 5%) were mounted on the front and rear sides of the placement head, respectively.

The measurements from the front camera were used to compare the effect of different laser power and compaction force values on tape inlet temperature since it might influence the resulting outlet temperature. A measurement line was placed at the visible nip point of the fifth tow in the thermal images as shown in Figure 3a. The average temperature during the steady portion of the placement course was calculated.

The rear camera was used to measure the temperature at the roller exit temperature distribution of the top surface of the newly placed tape. This was done by placing a measurement line at the centerline of the fifth tow in the thermal image as demonstrated in Figure 3b. The length of the measurement line was determined from a calibration image in which a ruler is positioned parallel to the roller exit line at 50 mm distance. The average temperature distribution on the line was calculated for frames where the process reaches steady state.

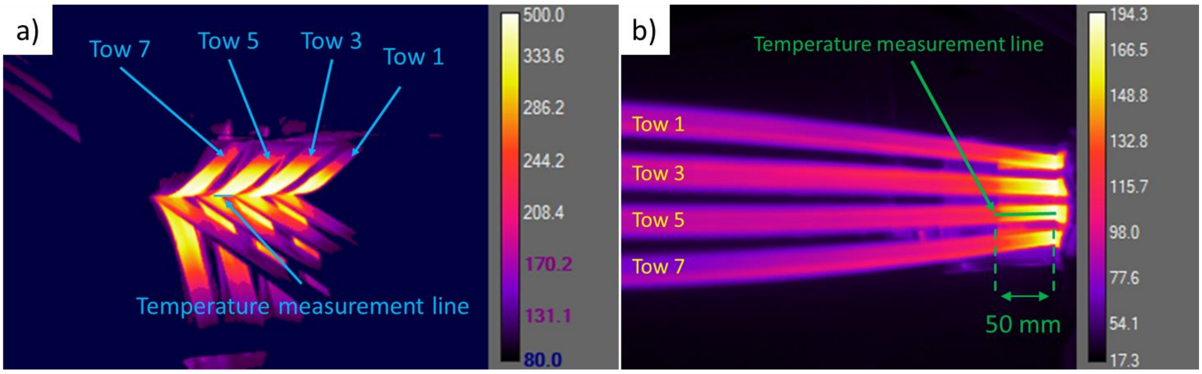

Figure 3. Thermal images and measurement lines from: a) the front thermal camera b) the rear thermal camera

2.3 Intimate Contact Measurement

To measure the intimate contact at the topmost interface of each specimen, cross-sectional micrographs were captured and analyzed. Samples were extracted from the fifth tow of each placement trial. Five 15 mm-long samples were cut past the first 300mm of the laminate as shown in Figure 4 to avoid the effects of the transient acceleration phase. The samples were embedded in mounting resin, ground and polished for high quality images. A Keyence VK-X1000 laser microscope was used to capture the cross-sectional micrographs of the topmost interface of the laminates. The whole width of each interface was captured by stitching approximately 55 images taken with a 50x-magnification lens to obtain high resolution images (0.55 µm/pixel).

A custom-made Matlab script was used to analyze the cross-sectional images with the methodology shown in Figure 5. Since the topmost interface was not a straight line for most of the images, a measurement curve was defined by selecting points manually. This initial curve was offset by one pixel in positive and negative vertical directions to create two additional curves (Figure 5b). This was done to ensure that the results were not affected by local features in the image. Then, a grayscale histogram was generated for each image. From this histogram, a threshold was determined with Otsu's threshold method [6] and the image was segmented such that the fiber-matrix mixture was distinguished from the voids (Figure 5c). After the segmentation procedure, the voids and the fiber-matrix mixture at the interface can be identified by the black and white pixels, respectively (Figure 5d). Finally, the degree of intimate contact was calculated as the ratio between the length of the white areas along the measurement curve and the total length of the measurement curve. The results from the three curves were averaged to obtain the final degree of intimate contact for each sample (Figure 5e).

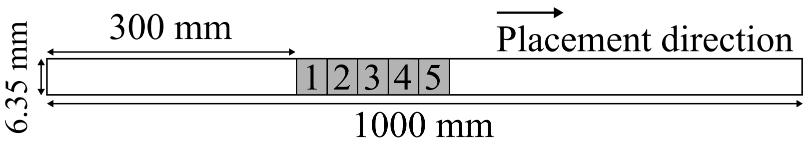

Figure 4. Extraction locations of five samples for intimate contact investigation.

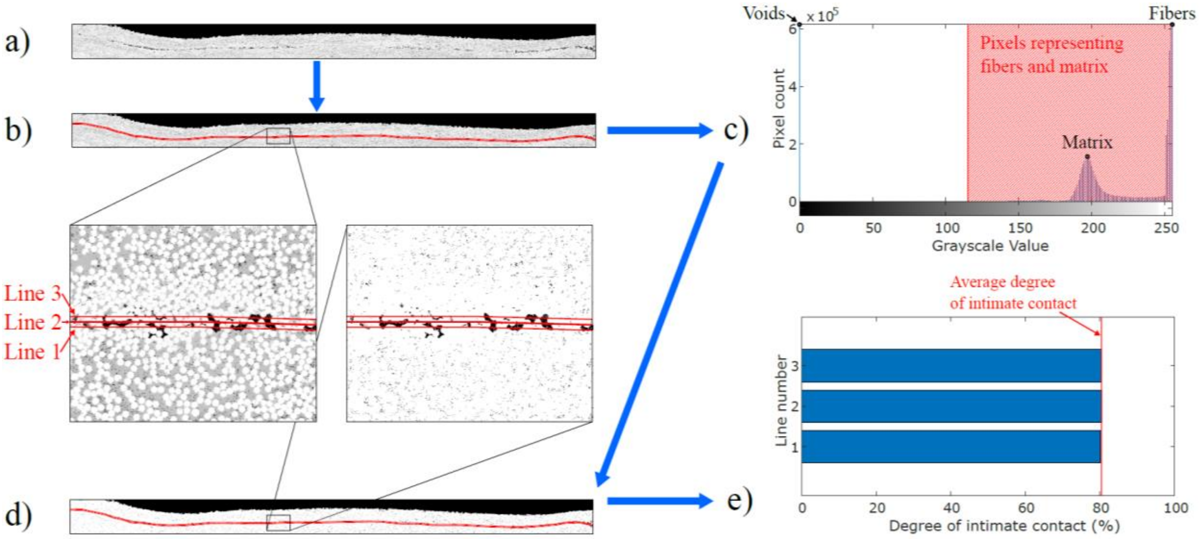

Figure 5. Methodology for intimate contact measurement at the topmost interface from cross-sectional images.

2.4 Analysis of Variance (ANOVA)

Two-way analysis of variance (ANOVA) method was applied on the results of the temperature measurements described in Section 2.2 and intimate contact measurements described in Section 2.3 to assess the effects of the laser power and compaction force quantitatively. The Matlab built-in function *anovan* was used for this purpose [7]. The outputs of this function were p-values for each process parameter. p-values smaller than 0.05 imply that the mean response of the specific parameter is different from the mean of all data within a confidence interval of 95 %.

3. RESULTS

3.1 Experimental Temperature History

The tape inlet temperatures just before the nip point at different laser power and compaction force values are shown in Figure 6. As the laser power increases, the tape inlet temperature increases for all compaction force levels. This is an expected result of the increased power density at the area illuminated by the laser. The effect of the compaction force is, however, not that obvious. A clear relation between the compaction force and the tape inlet temperature is not observed. This is also reflected in the results of the ANOVA; the effect of the laser power is statistically significant (p=0.0002) in contrast to the effect of the compaction force (p=0.2372). Recent studies proposed that the roller deformation due to increasing compaction force has an influence on the tape inlet temperature during the LAFP process [8]. The results in Figure 6 show that the roller deformation does not influence the observable tape inlet temperature more than the experimental scatter.

The temperature histories in the cooling region at the rear side of the roller are shown in Figure 7. The compaction force has an influence on the outlet temperature at every laser power. An increase in the compaction force results in a decrease in the temperature at the roller exit. The tape outlet temperature distribution for 500 N and 1000 N cases for each laser power are similar. However, when the compaction force is 100 N, a significant offset in temperature is observed, even though the inlet temperature is not higher than the others. When the effect of the laser power is examined, it can be seen that the exit temperature increases with increasing laser power if the compaction force is kept constant. However, the compaction force has such an importance that a tape placed with low compaction force can be warmer than a tape placed with a higher laser power and compaction force at the roller exit.

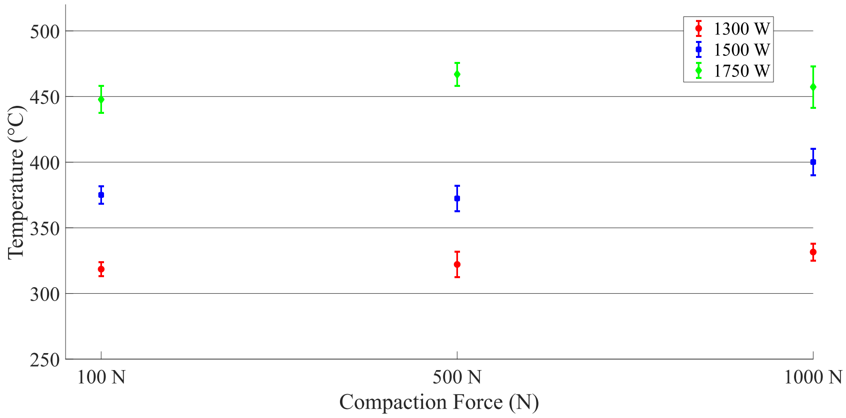

Figure 6. Average tape inlet temperatures for the fifth tow at each laser power and compaction force.

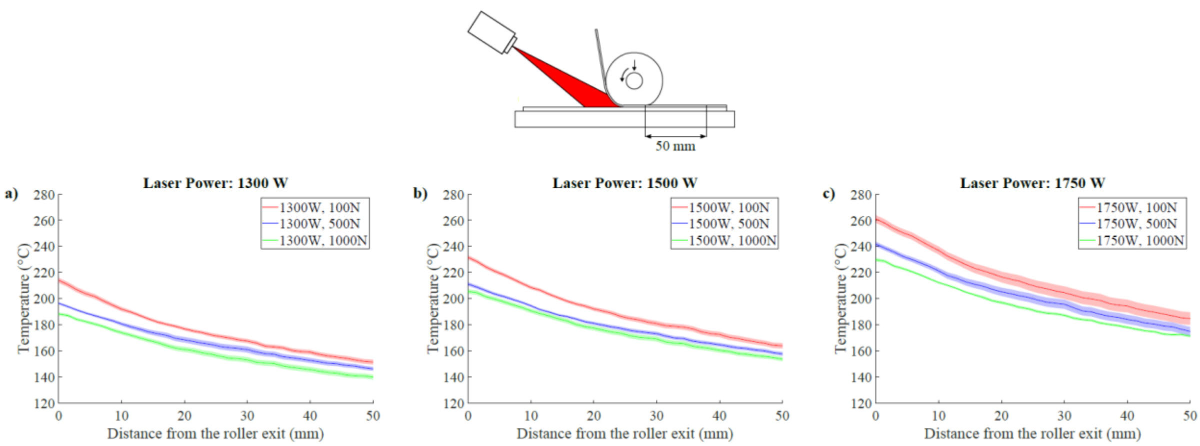

Figure 7. Average tape temperatures at the roller exit on the top surface of the fifth tow for different compaction forces and laser powers

3.2 Intimate Contact

The measured degree of intimate contact at the topmost interface for each parameter combination is shown in Figure 8. The ANOVA method is used again to quantify the effects of the laser power and the compaction force. The analysis shows that a variation of the laser power in the given range has a statistically insignificant effect ($p=0.5193$) on the final degree of intimate contact whereas the effect of the compaction force is statistically significant ($p=0.0232$). This is an interesting result since the temperature has been perceived as the most important process parameter to determine the part quality. Yet, the compaction force seems to drive the resulting degree of intimate contact independently of the temperature levels.

A compaction force of 100 N results in the lowest degree of intimate contact for all laser power levels. The degree of intimate contact increases as the compaction force is increased. In general, the difference between the 500 N and 1000 N is smaller than the difference between the 100 N and 500 N. The reason for that can be the nonlinear relationship between the applied force and the resulting pressure under the compaction roller. As the roller is deformed further, the contact area increases and limits the pressure [9].

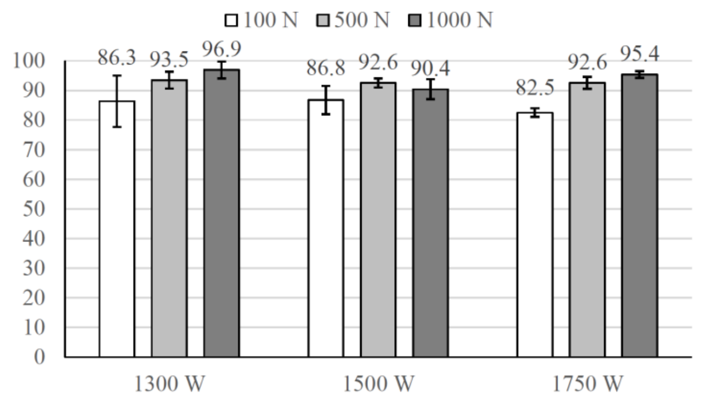

Figure 8. Average degree of intimate contact for each specimen.

4. DISCUSSION

The fact that the temperature at the roller exit is different for varying compaction forces indicates that the compaction force affects the thermal history during the LAFP process. The nip point temperature alone is not sufficient to describe the thermal history. Roller pressure and the resulting TCR affect the thermal history, meaning that it indirectly influences thermally driven phenomena such as healing or crystallinity evolution. This effect has not been clearly demonstrated for the LAFP process so far.

The change in the temperature history is in correlation with the degree of intimate contact at the topmost interface. As the degree of intimate contact decreases, the roller exit temperature increases and the tape stays at elevated temperatures for a longer duration. This agrees with the point of view that the air pockets at the interface hinder the through thickness heat transfer.

Importance of TCR has practical consequences. As the LAFP technology with in-situ consolidation matures, research in the field has expanded to more complex parts such as a fuselage panel [10], variable-stiffness wingbox [11] and a pressure vessel [12]. Complex tool shapes introduce convex or concave surfaces which result in a non-uniform pressure distribution under the compaction roller [13]. This may result in areas with insufficient intimate contact. The effects of TCR should be considered in such cases for an accurate thermal analysis of the process.

5. CONCLUSION AND FUTURE WORK

In this work, the effect of thermal contact resistance during LAFP was investigated experimentally. Samples with varying degrees of intimate contact were created by changing the compaction force at a constant laser power and process speed. The temperature at the roller exit was recorded with a thermal camera and cross-sectional micrographs were used to measure the degree of intimate contact. Samples with a lower degree of intimate contact were observed to be at a higher temperature at the roller exit and stay at higher temperature for longer duration. This suggests the effects of TCR can be observed during LAFP. Future work includes examining the effects of TCR numerically.

6. ACKNOWLEDGMENTS

This work is funded by European Regional Development Fund (ERDF) within the Smart Industry Fieldlab: ACM project under Grant No. KVW-00043. The authors would also like to thank Royal Netherlands Aerospace Center (NLR), especially Chris Groenendijk and Michiel Mandemaker, for the assistance with the LAFP machine.

7. REFERENCES

[1] Stokes-Griffin CM, Compston P. A combined optical-thermal model for near-infrared laser heating of thermoplastic composites in an automated tape placement process. Compos Part A Appl Sci Manuf 2015;75:104–15. doi:10.1016/j.compositesa.2014.08.006.

[2] Schaefer PM, Gierszewski D, Kollmannsberger A, Zaremba S, Drechsler K. Analysis and improved process response prediction of laser- assisted automated tape placement with PA-6/carbon tapes using Design of Experiments and numerical simulations. Compos Part A Appl Sci Manuf 2017;96:137–46. doi:10.1016/j.compositesa.2017.02.008.

[3] Weiler T, Emonts M, Wollenburg L, Janssen H. Transient thermal analysis of laser-assisted thermoplastic tape placement at high process speeds by use of analytical solutions. J Thermoplast Compos Mater 2018;31:311–38. doi:10.1177/0892705717697780.

[4] Barasinski A, Leygue A, Soccard E, Poitou A. Identification of non uniform thermal contact resistance in automated tape placement process. Int J Mater Form 2014;7:479–86. doi:10.1007/s12289-013-1144-9.

[5] Kollmannsberger A, Lichtinger R, Hohenester F, Ebel C, Drechsler K. Numerical analysis of the temperature profile during the laser-assisted automated fiber placement of CFRP tapes with thermoplastic matrix. J Thermoplast Compos Mater 2018;31:1563–86. doi:10.1177/0892705717738304.

[6] Otsu N. A Threshold Selection Method from Gray-Level Histograms. IEEE Trans Syst Man Cybern 1979;9:62–6. doi:10.1109/TSMC.1979.4310076.

[7] The MathWorks Inc. MATLAB and Statistics Toolbox Release 2017b 2017.

[8] Kok T. On the consolidation quality in laser assisted fiber placement: the role of the heating phase. University of Twente, 2018. doi:10.3990/1.9789036546065.

[9] Çelik O, Peeters D, Dransfeld C, Teuwen J. Intimate contact development during laser assisted fiber placement: Microstructure and effect of process parameters. Compos Part A Appl Sci Manuf 2020;134. doi:10.1016/j.compositesa.2020.105888.

[10] Rodriguez-Lence F, Martin MI, Fernandez Horcajo K. In-situ consolidation of integrated thermoplastic fuselage panels: The future in structural comercial aerocomposites. ECCM 2018 - 18th Eur. Conf. Compos. Mater., 2018.

[11] Oliveri V, Zucco G, Peeters D, Clancy G, Telford R, Rouhi M, et al. Design, manufacture and test of an in-situ consolidated thermoplastic variable-stiffness wingbox. AIAA J 2019;57:1671–83. doi:10.2514/1.J057758.

[12] Zaami A, Schäkel M, Baran I, Bor TC, Janssen H, Akkerman R. Temperature variation during continuous laser-assisted adjacent hoop winding of type-IV pressure vessels: An experimental analysis. J Compos Mater 2019. doi:10.1177/0021998319884101.

[13] Lichtinger R, Lacalle J, Hinterhölzl R, Beier U, Drechsler K. Simulation and experimental validation of gaps and bridging in the automated fiber placement process. Sci Eng Compos Mater 2015;22:131–48. doi:10.1515/secm-2013-0158.